

Photoelectron Trapping Mechanism for Horizontal Coupled Bunch Mode Growth in CESR

J. Rogers

We present a mechanism for horizontal coupled bunch mode growth (“anomalous antidamping”) in CESR. The effect is explained by the presence of photoelectrons trapped in the CESR beam chamber by the combined dipole magnetic field and the electrostatic leakage field of the distributed ion pumps. The motion of the beam modulates the trapped photoelectron charge density, which in turn deflects the beam, creating growth or damping and a tune shift for each coupled bunch mode. A simplified numerical model is used to calculate the growth rate and tune shift. Very preliminary predictions of this model are presented. These are in rough agreement with observation.

1 Introduction

An anomalous damping or growth of horizontal coupled bunch modes has long been observed in CESR [1]. The growth rates and tune shifts of these modes are a highly nonlinear function of beam current. The effect is known to be associated with the operation of the distributed ion pumps, as it is present only when these pumps are powered [2]. It is strongest at the intermediate currents encountered during CESR injection, and becomes dramatically weaker at higher currents. The absolute values of both the growth rate and tune shift are largest for the lowest frequency mode. They drop rapidly for higher frequency modes.

Because of its nonlinearity with current, and because it is present only when the distributed ion pumps are powered, this effect is not due to conducting boundaries in the CESR beam or pump chambers. Electrons or ions within the distributed ion pumps or ions drifting from the pumps to the beam region have all been suggested as the source of this nonlinearity. Here we present the hypothesis that slow electrons trapped in the CESR beam chamber are responsible. We show that photoelectrons from synchrotron radiation striking the beam chamber walls will be trapped in the combined dipole magnetic field and electrostatic leakage field from the distributed ion pumps, and calculate their interaction with the beam.

2 Photoelectron trapping

Slow photoelectrons in the CESR chamber will be confined to very small orbits in the horizontal plane by the 0.2 T magnetic field of the CESR dipoles. The quadrupole component of electrostatic leakage field from the distributed ion pump slots, calculated to be 2.1×10^4 V/m² at the center of the beam chamber [3], confines the electrons vertically. Positive ions are expelled by this field. The combination of these fields acts as a Penning trap for electrons, much like the ion pump itself. Because there is a horizontal dipole component of the pump

leakage field (320 V/m at the center of the beam chamber), the trapped electrons undergo an $\mathbf{E} \times \mathbf{B}$ drift down the length of the magnet, with a velocity of the order of 1.6×10^3 m/s. Thus a trapped electron is lost from the 6.5 m long magnets in about 2 ms. We will later show that electrons are removed by interactions with the beam on a far shorter time scale, so their drift velocity may be neglected. The cyclotron frequency of the trapped electrons is 5.6 GHz, so their horizontal motion is unimportant at the frequencies of the coupled bunch modes. The vertical motion, with frequencies of the order of 10 MHz or less, dominates the dynamics.

In addition to producing photoelectrons through synchrotron radiation, the beam has an essential role in trapping the electrons. An electron which is emitted from the chamber wall will soon collide with the chamber unless perturbed by the time-dependent force provided by the beam. Electrons which are deflected by the beam opposite their vertical velocities are trapped on orbits of lower amplitude. Other electrons are excited to higher amplitudes and may be lost in collisions with the beam chamber.

The magnitude of the impulse from the beam depends on the position of the position of the beam relative to the trapped electrons. Thus the oscillating beam position modulates the trapped charge density, which in turn drives the transverse oscillation of the beam. Coupled bunch modes are damped, driven unstable, or shifted in tune, depending on the phase of the trapped charge density relative to the beam motion.

3 Simulation

A simplified numerical model was produced to test the hypothesis that trapped photoelectrons could cause the observed growth or damping. In this model, we calculate the trajectories of photoelectrons moving under the influence of the electric field gradients of the distributed ion pumps, a bunched positron beam, and the other photoelectrons. Because several simplifying assumptions are used the calculated growth rates and tune shifts should be regarded as estimates.

We divide the beam chamber into $n_{x,max}$ slices along the x direction (i.e., from the inside to the outside of the ring). The height of the chamber, y_{wall} , is approximated as independent of x . In each time increment δt :

1. a photoelectron macroparticle is started in each x slice at $y = y_{wall}$ with vertical velocity $v_y = 0$;
2. the electric field gradient $\partial E_y / \partial y$ is calculated for each x slice;
3. y and v_y are updated for each macroparticle using the calculated $\partial E_y / \partial y$; and
4. any macroparticle for which $y \geq y_{wall}$ is removed.

No horizontal motion of the macroparticle is allowed because of the strong vertical magnetic field. All parameters are assumed to be independent of position along the length of the chamber, reducing the problem to two dimensions. An approximate model is used for the field gradients in which $\partial E_y / \partial y$ falls off as the square of the distance from the distributed pump slots and the beam, and the effect of the photoelectron macroparticles is to screen the

field due to the pump slots. Specifically,

$$\frac{\partial E_y}{\partial y} \approx -\frac{1}{2\pi\epsilon_0} \left(\frac{q_{slot} + \sum_{n=1}^{n_x} q_{pe,n}}{x^2} + \frac{q_{beam}}{(x_{beam} - x)^2} \right)$$

where q_{slot} is the effective linear charge density of the pump slots, $q_{pe,n}$ is the photoelectron linear charge density in slice n , q_{beam} is the linear charge density of the beam averaged over δt , and x is measured from the pump slots. The beam position x_{beam} is made to oscillate sinusoidally with amplitude A_x . The constants used in the simulation are listed in Tables 1 and 2.

Table 1: Simulation constants

$n_{x,max}$	Number of x slices	25
δx	Increment in x	1.6 mm
δt	Time increment	1.4 ns
A_x	Amplitude of horizontal betatron oscillation	4 mm

The time increment $\delta t = 1.4$ ns produced a trapped electron charge density vs. time that is consistent with that produced by smaller values of δt . The x increment δx was chosen to keep the computing time within reasonable bounds. The trapped photoelectrons were introduced only between the pump slots and the beam.

Table 2: Physical constants

y_{wall}	Beam chamber half-height	≈ 20 mm
x_{center}	Position of center of beam chamber	45.2 mm
Q_x	Horizontal tune	≈ 10.5
T_0	Revolution period	2.56 μ s
β_x	Average β function in dipole magnets	19 m
p	Beam momentum	5.3 GeV/c
L_{slot}	Total pump slot length	408 m
q_{slot}	Effective slot linear charge density	4.79×10^{-9} C/m
R_{pe}	Photoemission rate	0.92 m^{-1}

All of the physical constants used in the simulation are based on measured quantities except R_{pe} , the photoelectron charge injected per unit time, length, and beam current. No attempt was made to calculate or directly measure this quantity. It was treated as a free parameter, and was adjusted so that the maximum growth rate for the 7 bunch pattern occurred 5 mA as experimentally observed. It was then held fixed at this value for all simulations. No other free parameters were used, and no other changes of any sort were made to the original numerical model to bring it in closer agreement with experimental observations.

4 Simulation results

4.1 Time dependence of trapped charge density

The calculated photoelectron charge density as a function of time for the 7 bunch pattern is shown in Fig. 1. The horizontal scale is in units of $\delta t = 1.4$ ns. The abrupt loss of trapped charge following each bunch passage is clearly seen, as is the slow variation due to the horizontal beam oscillation.

The reason that the instability growth rate falls off rapidly at higher beam currents is apparent from these plots. The rate at which photoelectrons are injected into the beam chamber is proportional to the synchrotron radiation flux, which is in turn proportional to the beam current. When the average photoelectron charge density is sufficient to completely screen the pump leakage field, no more electrons can be trapped. The charge density reaches an approximately constant level, extinguishing the variation needed to drive the beam.

The trapped photoelectron density depends strongly on the details of the bunch pattern. The effect of a very small gap in the bunch pattern can be seen in the sudden drop every turn (1830 increments) in Fig. 1b (the interval between bunches 7 and 1 is 378 ns as opposed to 364 ns for all other bunches). The characteristic recovery time of the photoelectron charge is of the order of 50 ns, as shown in Fig. 2, where the data of Fig. 1d are plotted on a finer time scale.

4.2 Current dependence of growth rate and tune shift

To obtain the coupled bunch growth rate α_x and tune shift $\delta\omega_x$, we calculated the force on the beam at the frequency at which it is driven. If A_{pe} and B_{pe} are the sine and cosine Fourier coefficients of the photoelectron density at that frequency,

$$\alpha_x = \left(\frac{\bar{\beta}_x}{2T_0} \right) \left(\frac{eB_{pe} L_{slot}}{2\pi\epsilon_0 x_{center} pc A_x} \right)$$
$$\delta\omega_x = - \left(\frac{\bar{\beta}_x}{2T_0} \right) \left(\frac{eA_{pe} L_{slot}}{2\pi\epsilon_0 x_{center} pc A_x} \right)$$

We used only the last 6 CESR turns of simulation data to calculate A_{pe} and B_{pe} . We approximated β_x by its average $\bar{\beta}_x$ throughout the dipole magnets. The growth rates and tune shifts for the 7 bunch, 9 bunch, and 9×2 bunch patterns are shown in Figures 3, 4, and 5. In the 9×2 pattern there are 9 trains of two bunches each, with a 28 ns interval between the two bunches in a train. Because the characteristic recovery time of the photoelectron charge is longer than the interval between bunches, the bunches within a train are expected to act partially coherently. Comparison of Figs. 4 and 5 shows that the presence of two bunches in a train pushes the maximum growth rate and tune shift to lower current per bunch, as is observed experimentally.

4.3 Frequency dependence of growth rate and tune shift

To determine the dependence of the growth rate and tune shift on the coupled-bunch frequency we followed the same procedure for coupled bunch modes with frequencies of $f_0/2$, $3f_0/2$, and $5f_0/2$, where $f_0 = 390$ kHz is the CESR revolution frequency. We used the 7

bunch pattern with 3 mA/bunch. The results are shown in Table 3. The magnitude of both the growth rate and tune shift fall off rapidly with increasing frequency, in qualitative agreement with observation.

Table 3: Frequency dependence of growth rate and tune shift

Coupled bunch mode frequency	α_x (s^{-1})	$\delta\omega_x/2\pi$ (Hz)
$f_0/2$	291.1	78.2
$3f_0/2$	-37.8	0.7
$5f_0/2$	2.2	2.0

5 Concluding comments

The photoelectron trapping mechanism presented here provides a full qualitative understanding of anomalous antidamping in CESR. It explains why the instability occurs only when the pumps are powered. Because the time-averaged electric field from the photoelectrons is primarily horizontal, it is understood why the instability is horizontal. The rapid decrease in the growth rate at higher currents is explained as a saturation of the trapped photoelectron charge due to the higher synchrotron radiation flux. The recovery time in the model explains why the current at which the maximum growth rate occurs depends on the total current in a train of bunches rather than on the current per bunch.

The numerical model provides estimates of growth rates which are in approximate agreement with observations in spite of a number of simplifying assumptions. For example, the calculated growth rate for the 7 bunch pattern at 4 mA/bunch is 740 s^{-1} , while the observed rate is 520 s^{-1} [1]. The numerical model reproduces the observed behavior of the tune shift, which changes sign at the same current at which the growth rate starts to diminish, and predicts that the magnitude of the growth rate falls rapidly with frequency.

An improved numerical model is currently being produced by T. Holmquist in cooperation with the author. We intend to include the variation of y_{wall} with x and to improve the calculation of the electromagnetic fields. We wish to address several remaining questions:

1. Can we account for the observed difference between e^+ and e^- growth rates?
2. What is the predicted variation of growth rate with pump anode voltage?
3. Will this effect be observed in other electron storage rings with similar pumps?
4. What is the predicted growth rate for the CESR Phase 3 bunch pattern?
5. What is the effect of gaps in the bunch pattern?
6. Can we directly calculate the photoemission rate?

One point of particular concern is the observation that the $m = 1$ vertical head-tail mode appears to be stabilized by the operation of the distributed ion pumps [2]. We note that the peak of the frequency spectrum for this mode occurs at approximately 2.4 GHz, with substantial spectral density at the 5.6 GHz cyclotron frequency of the trapped photoelectrons. The photoelectrons may be absorbing energy from this mode before being lost by collision

with the chamber. We wish to understand this process before making irreversible changes to the CESR ion pumps meant to reduce the coupled bunch growth rate.

The author wishes to thank the many members of the CESR Operations Group, with special thanks to M. Billing, for stimulating discussions on observations and possible causes of the anomalous antidamping effect. This work was supported by the National Science Foundation.

References

- [1] L.E. Sakazaki, R.M. Littauer, R.H. Siemann, and R.M. Talman, *IEEE Trans. Nucl. Sci.* **32** (1985) 2353-2355; L.E. Sakazaki, Ph.D. thesis, Cornell Univ. (1985).
- [2] R. Littauer, Cornell LNS report CLNS 88/847 (1988).
- [3] D. Sagan and J.J. Welch, Cornell LNS report CBN 92-01 (1992).

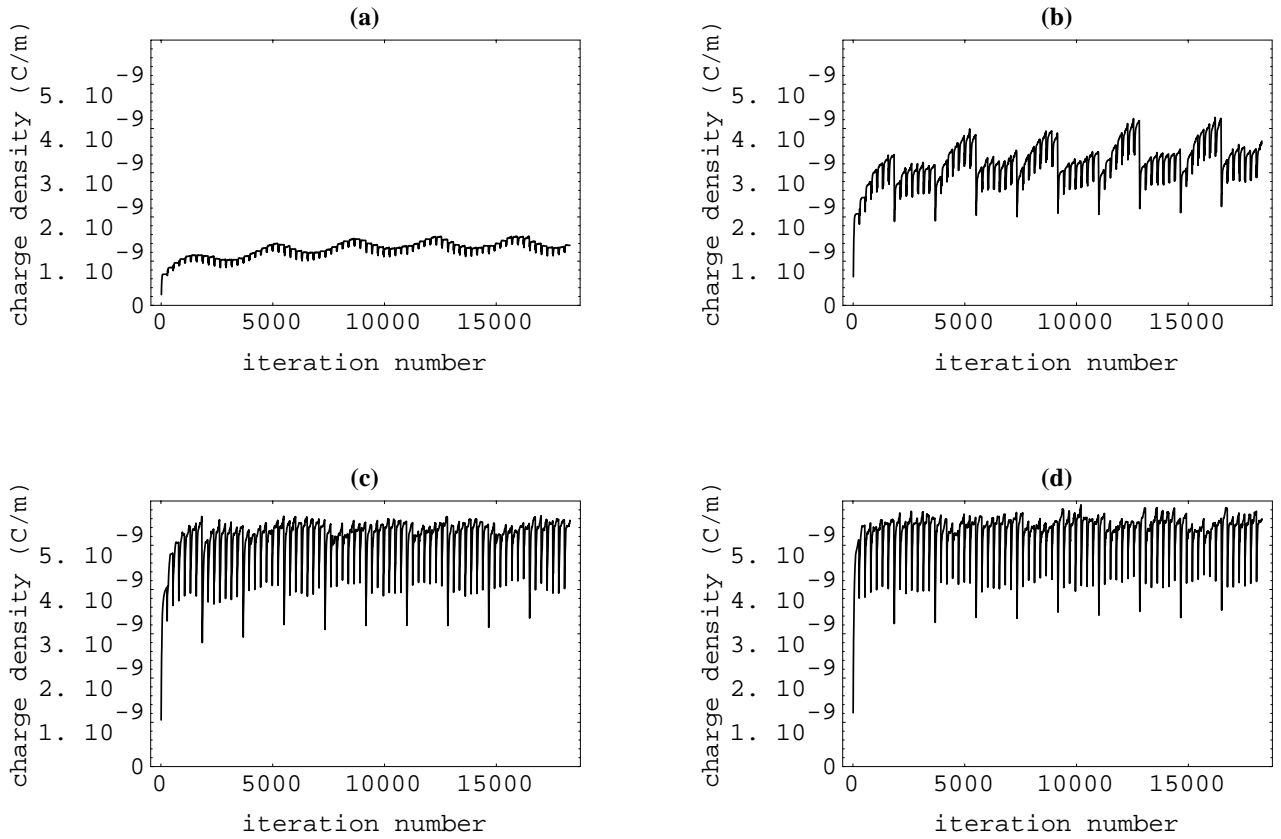


Figure 1: Calculated linear charge density vs. time of the trapped photoelectrons for the 7 bunch pattern. The horizontal scale is in units of the 1.4 ns time increment used in the simulation. The total time is 10 CESR revolutions. The beam is moving horizontally with frequency $f_0/2$. The beam currents are: (a) 3 mA/bunch; (b) 5 mA/bunch; (c) 6 mA/bunch; and (d) 7 mA/bunch.

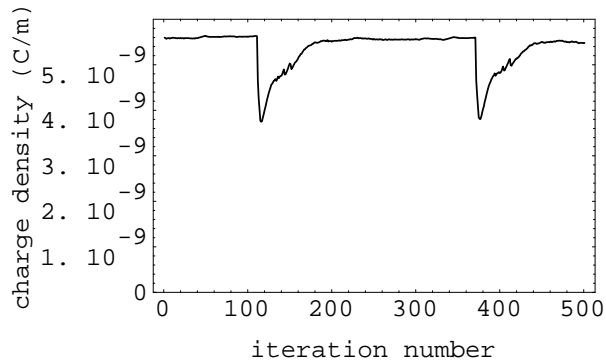


Figure 2: Calculated linear charge density vs. time of trapped photoelectrons. This is the data of Fig. 1d plotted on a finer time scale. The horizontal scale is in units of 1.4 ns.

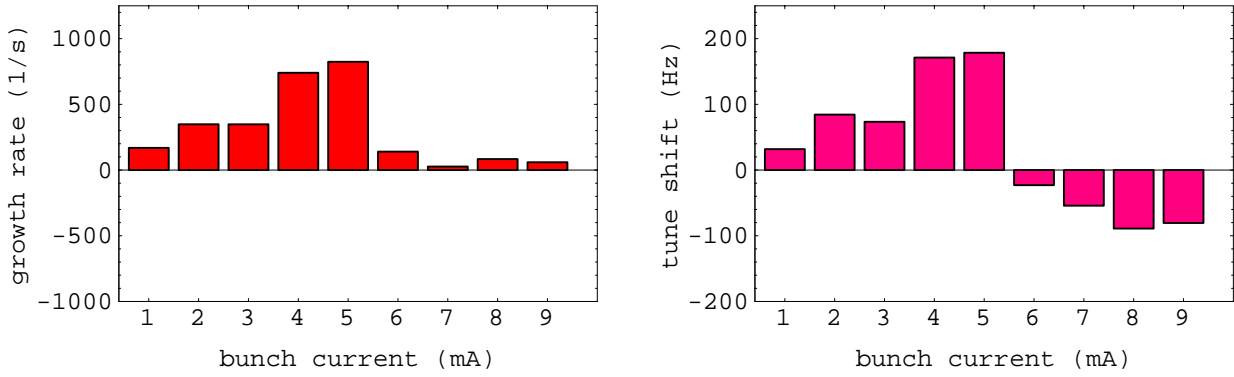


Figure 3: Calculated growth rate and tune shift vs. bunch current for 7 bunches in CESR.

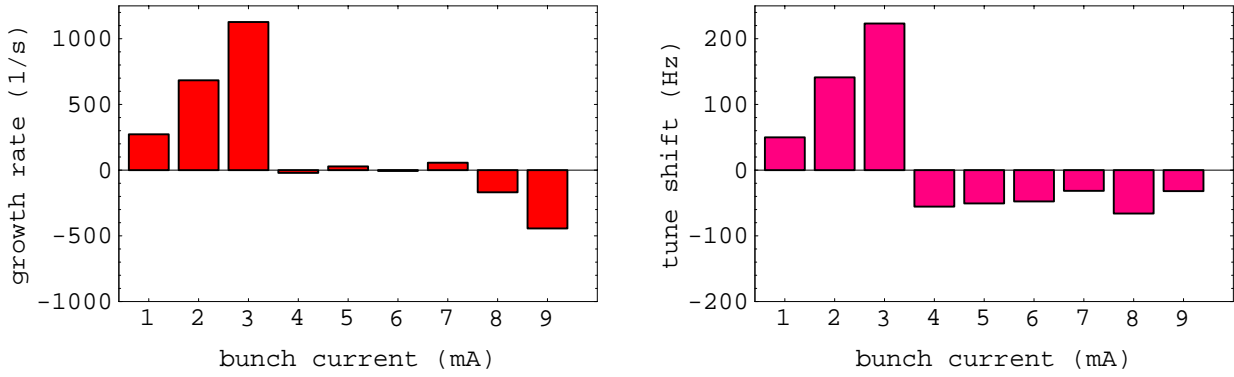


Figure 4: Calculated growth rate and tune shift vs. bunch current for 9 bunches in CESR.

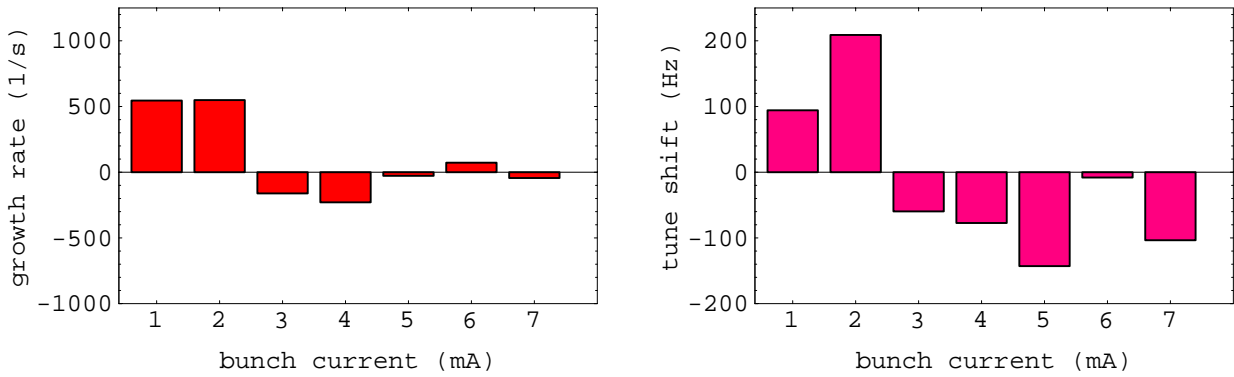


Figure 5: Calculated growth rate and tune shift vs. bunch current for 9 trains of 2 bunches each in CESR.